

## Local extrema for energy in two-phase optimal design problems\*

PETAR KUNŠTEK AND MARKO VRDOLJAK<sup>†</sup>

*Department of Mathematics, Faculty of Science, University of Zagreb, Croatia*

Received March 30, 2023; accepted October 13, 2023

---

**Abstract.** We consider conductivity optimal design problems for two isotropic phases with prescribed amounts, optimizing the energy functional. We analyze optimality conditions obtained by shape calculus, in the spherically symmetric case for simple radial designs, such that the interface between two given isotropic phases consists of a single sphere. Every such design satisfies the first-order optimality condition. By using classical Fourier analysis techniques we are able to express and analyze the second-order optimality conditions. This implies that for any outer heat source, considered simple designs cannot give local minima of the energy functional. Two examples are presented, showing that the presented approach gives a complete answer whether a considered critical design is a saddle point, or the Lagrangian satisfies the negative coercivity condition in  $H^{\frac{1}{2}}$  norm of normal perturbation on the interface. In the latter case, we numerically confirm the appearance of local maxima, different from the global one.

**AMS subject classifications:** 49Q10, 49K20, 80M50

**Keywords:** optimal design, shape derivative, second-order shape derivative, optimality conditions

---

### 1. Introduction

In optimal design problems one is seeking for an arrangement of two (or more) given materials, such that the mixture has some optimal properties. Classically, this optimality is expressed in terms of minimization of some integral functional.

We consider composites made of two isotropic materials with the (heat) conductivities  $\alpha$  and  $\beta$ , with  $0 < \alpha < \beta$ , in a given open, bounded and Lipschitz set  $\Omega \subseteq \mathbb{R}^d$ . Let us denote by  $\Omega_\alpha$  the set occupied by the first phase, and  $\Omega_\beta := \Omega \setminus \Omega_\alpha$ . Therefore, the conductivity can be written as  $a = \chi_\alpha \alpha + (1 - \chi_\alpha) \beta$ , where  $\chi_\alpha$  is the characteristic function of the set  $\Omega_\alpha$ .

The state function  $u$  represents the temperature of the body, and it is uniquely determined by

$$\begin{cases} -\operatorname{div}(a \nabla u) = f \\ u \in H_0^1(\Omega), \end{cases} \quad (1)$$

---

\*This work has been supported in part by the Croatian Science Foundation under the project IP-2018-01-3706.

<sup>†</sup>Corresponding author. *Email addresses:* `petar@math.hr` (P. Kunštek), `marko@math.hr` (M. Vrdoljak)

as long as  $a$  is measurable, and  $f \in H^{-1}(\Omega)$ . The aim is to maximize the energy functional (if  $f \in H^{-1}(\Omega)$ , the first integral should be replaced by the dual mapping)

$$J(\Omega_\alpha) = \int_{\Omega} f u \, d\mathbf{x} = \int_{\Omega} a |\nabla u|^2 \, d\mathbf{x} \rightarrow \max, \quad (2)$$

under the volume constraint on the amounts of original phases. More precisely, we assume that the amount of the first phase is fixed to  $q_\alpha \in \langle 0, \text{vol}(\Omega) \rangle$ :

$$\text{vol}(\Omega_\alpha) = \int_{\Omega} \chi_\alpha \, d\mathbf{x} = q_\alpha. \quad (3)$$

Let us emphasize that domain  $\Omega$  is fixed, and we are looking for an optimal arrangement of two given isotropic phases, i.e. an optimal set  $\Omega_\alpha$  occupied by the first phase.

It is well known [22, 29, 18] that this problem has a solution in the spherically symmetric case, where  $\Omega$  is a ball or an annulus, and  $f$  is a radial function. More precisely, an application of saddle point theory leads to a unique solution, except in some singular cases. However, to obtain this result, as a first step one should introduce a proper relaxation of the optimal design problem via homogenization theory [22]. This procedure consists in introducing generalized materials, which are mixtures of the original phases on the micro-scale. The analogous minimization problem shows different behaviour since one cannot avoid generalized materials to reach the minimum [22, 6]. Generally, this situation can be fixed by introducing additional regularizing terms to the functional, e.g. the perimeter of the interface between phases should be added [4, 12].

Even for the simplest, spherically symmetric case, although the maximizer is unique, the question of its stability arises. Furthermore, it is interesting to see whether there exist some other local extrema. We shall approach these questions via shape calculus, which has been successfully applied in [7] to the same problem, but with a constant right-hand side  $f = 1$ . There, after expressing the first- and second-order shape derivatives, the author uses the Fourier series expansion technique to check the sign of second-order variations for critical designs in the case of simple radial designs, such that the interface between two given isotropic phases consists of a single sphere. However, the calculations are tied to the specific choice  $f = 1$ , and in such a case, there occur no local extrema, apart from the well-known global maximizer in which one places a better conductor within an inner ball [22]. Our aim in this paper is to study a general right-hand side  $f$ .

However, the application of shape differentiation for determining local extrema is not straightforward, as explained in [11]. In a finite dimensional optimization problem, the stability of a critical point is equivalent to positivity of any second-order variation, but in infinite dimensions, this is not the case. The stability question in optimal design problems was first raised in [13]. A profound study of stability in shape optimization is presented in [10] (see also [9, 2]), with a wide literature overview. The problem lies in the fact that the coercivity is given in a weaker norm than the norm in which the functional is twice differentiable. The solution by [10] is to prove a precise bound on the perturbation of the second-order shape derivative with respect to normal perturbations. That kind of results is well known for optimal

design problems in which one looks for an optimal domain  $\Omega$ , but for homogeneous bodies, which could not be easily applied to our problem with two materials. Since this is still an open problem, in this paper we numerically check the appearance of local extrema.

Spherically symmetric problems are of special interest since the optimal (global) design can be explicitly found by solving an ordinary differential equation [22, 29, 18]. If we denote by  $\Gamma$  the interface between the two phases, then, generally, the optimal solution has a nice property that  $\Gamma$  is a sphere, or a union of spheres, (compactly) embedded in  $\Omega$ . In accordance with this, we take the following assumption in this paper: sets  $\Omega_\alpha$  and  $\Omega_\beta$  are open sets with a Lipschitz boundary, and the interface  $\Gamma$  between them is embedded in  $\Omega$ . Therefore, we have  $\Omega = \Omega_\alpha \dot{\cup} \Omega_\beta \dot{\cup} \Gamma$ .

Shape calculus is introduced by Hadamard [14]. We follow the displacement field method studied by Murat and Simon [21], see also [3, 15]. In this approach, for a given arrangement of two given phases, as above, we consider its small perturbation by the homeomorphism  $\Phi_\theta := \text{Id} + \theta$  for some small  $\theta \in W_0^{k,\infty}(\Omega; \mathbb{R}^d)$ . Such homeomorphism defines perturbed characteristic function  $\chi_\alpha \circ \Phi_\theta$  of the first phase, and we shall denote the corresponding state function by  $u(\theta)$ .

Consequently, the perturbed energy functional is well-defined on some small neighbourhood of zero in  $W_0^{k,\infty}(\Omega; \mathbb{R}^d)$  by

$$\mathcal{J}(\theta) := J(\Phi_\theta(\Omega_\alpha)),$$

and the shape differentiability of the energy functional  $J$  at  $\Omega_\alpha$  is introduced as the Fréchet differentiability of the functional  $\mathcal{J}$  at zero, with notation

$$J'(\Omega_\alpha; \theta) := \mathcal{J}'(\mathbf{0}; \theta).$$

Actually, it suffices to take  $k = 1$ , and if  $\Gamma$  is  $C^2$  and  $f \in H^1(\Omega)$ , we have the following formula [5, 25, 24, 17] (for the same setting but with a different functional, see [16, 20, 1]):

$$J'(\Omega_\alpha; \theta) = \int_\Gamma \theta \cdot \mathbf{n} \left[ 2a \left| \frac{\partial u}{\partial \mathbf{n}} \right|^2 - a |\nabla u|^2 \right] dS, \tag{4}$$

where  $\mathbf{n}$  denotes the unit normal to  $\Gamma$ , oriented as the outer normal to  $\Omega_\alpha$ . The bracket  $[[\cdot]]$  denotes the jump on the interface  $\Gamma$ , in the direction  $\mathbf{n}$ : if  $h = h_\alpha \chi_\alpha + h_\beta (1 - \chi_\alpha)$ , then  $[[h]] = h_\alpha|_\Gamma - h_\beta|_\Gamma$ .

If the functional  $\mathcal{J}$  possesses the second-order Fréchet differential at zero, we say that  $J$  is second-order shape differentiable at  $\Omega_\alpha$ , and we use the notation

$$J''(\Omega_\alpha; \theta, \psi) := \mathcal{J}''(\mathbf{0}; \theta, \psi) = \lim_{t \rightarrow 0} \frac{\mathcal{J}'(t\psi; \theta) - \mathcal{J}'(\mathbf{0}; \theta)}{t}.$$

We shall use the well-known structure theorems [12], see also [15, 28]. Speaking in terms of the problem that we consider, where  $\Omega_\alpha$  is the set under perturbation, and the interface  $\Gamma$  is compactly embedded in  $\Omega$ , the first structure theorem states that for a shape differentiable function  $J$  and some  $C^{k+1}$  set  $\Omega_\alpha$ , there exists a continuous linear form  $l_1^J$  on  $C^k(\Gamma)$  such that

$$J'(\Omega_\alpha; \theta) = l_1^J(\theta|_\Gamma \cdot \mathbf{n}),$$

for any  $\boldsymbol{\theta} \in C_0^\infty(\Omega; \mathbb{R}^d)$ . By the second structure theorem [23], if  $J$  is twice shape differentiable at some  $C^{k+2}$  set  $\Omega_\alpha$ , then there exists a continuous bilinear form  $l_2^J$  on  $C^k(\Gamma) \times C^k(\Gamma)$  such that for any  $\boldsymbol{\psi}, \boldsymbol{\theta} \in C_0^\infty(\Omega; \mathbb{R}^d)$

$$J''(\Omega_\alpha; \boldsymbol{\theta}, \boldsymbol{\psi}) = l_2^J(\boldsymbol{\theta}|_\Gamma \cdot \mathbf{n}, \boldsymbol{\psi}|_\Gamma \cdot \mathbf{n}) + l_1^J(Z_{\boldsymbol{\theta}, \boldsymbol{\psi}}),$$

where  $Z_{\boldsymbol{\theta}, \boldsymbol{\psi}} = D_\Gamma \mathbf{n} \boldsymbol{\psi}_\Gamma \cdot \boldsymbol{\theta}_\Gamma - \nabla_\Gamma(\boldsymbol{\psi} \cdot \mathbf{n}) \cdot \boldsymbol{\theta}_\Gamma - \nabla_\Gamma(\boldsymbol{\theta} \cdot \mathbf{n}) \cdot \boldsymbol{\psi}_\Gamma$  on  $\Gamma$ . Here for a given  $C^1$  scalar function  $g$  and a vector function  $\mathbf{g}$ , defined on  $\Gamma$ , we use the following notations for the tangential component and the tangential gradient on  $\Gamma$ , respectively:

$$\begin{aligned} \mathbf{g}_\Gamma &= \mathbf{g} - (\mathbf{g} \cdot \mathbf{n}) \cdot \mathbf{n} \\ \nabla_\Gamma g &= \nabla \tilde{g} - (\nabla \tilde{g} \cdot \mathbf{n}) \cdot \mathbf{n}, \end{aligned}$$

where  $\tilde{g}$  denotes any  $C^1$  extension of  $g$  on some neighborhood of  $\Gamma$  [15, Subsection 5.4.3]. By  $D_\Gamma \mathbf{g}$  we denote the matrix with the  $i$ -th row  $(\nabla_\Gamma g_i)^\top$ , where  $g_i$  is the  $i$ -th component of  $\mathbf{g}$ . In what follows, we shall also use notation  $\operatorname{div}_\Gamma \mathbf{g} = \operatorname{tr} D_\Gamma \mathbf{g}$  for the tangential divergence of  $\mathbf{g}$  on  $\Gamma$ .

The paper is organized as follows. The second section presents the calculation of the second-order shape derivative of the energy functional. The rest of the paper deals with the spherically symmetric case in two dimensions and simple designs such that the interface  $\Gamma$  consists of just one sphere. In the third section, we express the first- and the second-order optimality condition via shape calculus in explicit expressions in terms of the heat flux  $\boldsymbol{\sigma} = a \nabla u$ , which determines possible critical shapes, as well as the corresponding Lagrange multipliers generated from the volume constraint. The second-order optimality condition is analyzed via Fourier analysis. If the interface consists of one circle, the complete answer whether a critical shape gives local extrema or not is presented in Corollary 1. The fourth section demonstrates an application of the presented results, while the last section confirms numerically the presence of local extrema, qualitatively much different from the global one.

## 2. Second-order shape derivative

To calculate the second-order shape derivative of the energy functional  $J$  we shall use the formula [26]

$$J''(\Omega_\alpha; \boldsymbol{\theta}, \boldsymbol{\psi}) = (J'(\Omega_\alpha; \boldsymbol{\theta}))'(\Omega_\alpha; \boldsymbol{\psi}) - J'(\Omega_\alpha; \nabla \boldsymbol{\theta} \boldsymbol{\psi}). \quad (5)$$

In this calculation, the local derivative  $u'$  of  $u$  appears, which is defined on each compact set  $K \subset \subset \Omega_\alpha \cup \Omega_\beta$  as the Fréchet differential at zero of  $\boldsymbol{\theta} \rightarrow u(\boldsymbol{\theta})|_K$ , from some  $W^{k, \infty}(\mathbb{R}^d; \mathbb{R}^d)$  neighbourhood of zero to  $H^1(K)$ . Its directional derivative at zero in direction  $\boldsymbol{\theta}$  will be denoted by  $u'(\boldsymbol{\theta})$ .

In the case of boundary value problem (1), for given  $\boldsymbol{\theta} \in W^{2, \infty}(\mathbb{R}^d; \mathbb{R}^d)$ ,  $\Gamma$  of class  $C^3$  and  $f \in H^1(\Omega)$ ,  $u'(\boldsymbol{\theta})$  belongs to  $L^2(\Omega)$ , and is uniquely determined by ([25], [17],

or a similar calculation in [1])

$$\left\{ \begin{array}{ll} \Delta u' = 0 & \text{in } \Omega_\alpha \cup \Omega_\beta \\ \llbracket u' \rrbracket = \frac{\alpha - \beta}{\alpha\beta} (\boldsymbol{\sigma} \cdot \mathbf{n}) \phi & \text{on } \Gamma \\ \llbracket a \nabla u' \cdot \mathbf{n} \rrbracket = (\alpha - \beta) \operatorname{div}_\Gamma (\phi \nabla_\Gamma u) & \text{on } \Gamma \\ u' = 0 & \text{on } \partial\Omega. \end{array} \right. \quad (6)$$

where  $\phi$  denotes  $\boldsymbol{\theta} \cdot \mathbf{n}$ , and  $\boldsymbol{\sigma} = a \nabla u$  is the heat flux.

For the first term in formula (5), we start from the boundary expression (4), and use [21, Section IV.4.4] (see also [15, Theorem 5.4.17]). In what follows, we use the notation

$$\gamma = 2a \left| \frac{\partial u}{\partial \mathbf{n}} \right|^2 - a |\nabla u|^2 = a \left| \frac{\partial u}{\partial \mathbf{n}} \right|^2 - a |\nabla_\Gamma u|^2.$$

A straightforward calculation leads to the formula

$$\begin{aligned} J''(\Omega_\alpha; \boldsymbol{\theta}, \boldsymbol{\psi}) &= \int_\Gamma \boldsymbol{\theta} \cdot \mathbf{n}'(\boldsymbol{\psi}) \llbracket \gamma \rrbracket dS \\ &+ \int_\Gamma \boldsymbol{\theta} \cdot \mathbf{n} \left[ 2a \frac{\partial u}{\partial \mathbf{n}} \frac{\partial u'(\boldsymbol{\psi})}{\partial \mathbf{n}} + 4a \frac{\partial u}{\partial \mathbf{n}} \nabla u \cdot \mathbf{n}'(\boldsymbol{\psi}) - 2a \nabla_\Gamma u \cdot \nabla_\Gamma u'(\boldsymbol{\psi}) \right] dS \\ &+ \int_\Gamma \boldsymbol{\psi} \cdot \mathbf{n} \left\{ H \boldsymbol{\theta} \cdot \mathbf{n} \llbracket \gamma \rrbracket + \frac{\partial}{\partial \mathbf{n}} (\boldsymbol{\theta} \cdot \mathbf{n} \llbracket \gamma \rrbracket) \right\} dS \\ &- \int_\Gamma \nabla \boldsymbol{\theta} \boldsymbol{\psi} \cdot \mathbf{n} \llbracket \gamma \rrbracket dS, \end{aligned}$$

where  $H = \operatorname{div}_\Gamma \mathbf{n}$  denotes the mean curvature of  $\Gamma$ . By using the identity  $\mathbf{n}'(\boldsymbol{\psi}) = -\nabla_\Gamma (\boldsymbol{\psi} \cdot \mathbf{n})$ , and noting that

$$Z_{\boldsymbol{\theta}, \boldsymbol{\psi}} = -\nabla_\Gamma (\boldsymbol{\psi} \cdot \mathbf{n}) \cdot \boldsymbol{\theta}_\Gamma + (\boldsymbol{\psi} \cdot \mathbf{n}) \nabla (\boldsymbol{\theta} \cdot \mathbf{n}) \cdot \mathbf{n} - (\nabla \boldsymbol{\theta}^t \mathbf{n}) \cdot \boldsymbol{\psi},$$

we transform the above expression to

$$\begin{aligned} J''(\Omega_\alpha; \boldsymbol{\theta}, \boldsymbol{\psi}) &= \int_\Gamma Z_{\boldsymbol{\theta}, \boldsymbol{\psi}} \llbracket \gamma \rrbracket dS + \int_\Gamma (\boldsymbol{\psi} \cdot \mathbf{n}) (\boldsymbol{\theta} \cdot \mathbf{n}) \left\{ H \llbracket \gamma \rrbracket + \frac{\partial}{\partial \mathbf{n}} \llbracket \gamma \rrbracket \right\} dS \\ &+ \int_\Gamma \boldsymbol{\theta} \cdot \mathbf{n} \left[ 2a \frac{\partial u}{\partial \mathbf{n}} \frac{\partial u'(\boldsymbol{\psi})}{\partial \mathbf{n}} - 4a \frac{\partial u}{\partial \mathbf{n}} \nabla u \cdot \nabla_\Gamma (\boldsymbol{\psi} \cdot \mathbf{n}) \right. \\ &\left. - 2a \nabla_\Gamma u \cdot \nabla_\Gamma u'(\boldsymbol{\psi}) \right] dS. \end{aligned} \quad (7)$$

**Remark 1.** *There are numerous approaches and techniques available for calculating first-order shape derivatives. When computing second-order shape derivatives in a broader context, the second-order shape derivative of the state function, as demonstrated in [2], can be employed. One key advantage of this method is its applicability to more general functionals. It does not rely on the specific structure of the functional or the feasibility of using adjoint methods [8, 27].*

**Remark 2.** For the previous results regarding the shape derivatives, we have assumed that the right-hand side  $f$  belongs to  $H^1(\Omega)$ . This is important for showing that the map

$$\boldsymbol{\theta} \mapsto f \circ \Phi_{\boldsymbol{\theta}} : W_0^{1,\infty}(\Omega; \mathbb{R}^d) \rightarrow H^{-1}(\Omega)$$

is shape differentiable, which fails to be true even in the case  $f \in L^2(\Omega)$ .

However, if we assume that  $f \in L^2(\Omega)$ , and there exists an open set  $\Omega_{\Gamma} \subset \Omega$  such that  $\Gamma \subset \Omega_{\Gamma}$  and  $f \in H^1(\Omega_{\Gamma})$ , one can show that the energy functional  $\boldsymbol{\theta} \mapsto \mathcal{J}(\boldsymbol{\theta}) : W_0^{1,\infty}(\Omega_{\Gamma}) \rightarrow \mathbb{R}$  is again shape differentiable with the same shape derivatives (4) and (7).

### 3. Optimality conditions for balls in spherically symmetric problem

In the sequel, let  $\Omega$  be a ball  $B(\mathbf{0}, R) \subseteq \mathbb{R}^2$ , and  $f$  a radial function. Our aim is to formulate the first- and the second-order optimality conditions for simple radial designs such that the interface  $\Gamma$  consists of just one sphere  $\partial B(\mathbf{0}, \hat{r})$ , where  $0 < \hat{r} < R$ . In other words, we consider only two possible designs: either  $\Omega_{\alpha}$  or  $\Omega_{\beta}$  equals  $B(\mathbf{0}, \hat{r})$ . To distinguish between these two cases, we introduce parameter  $\varepsilon$ : we take  $\varepsilon = 1$  if  $\Omega_{\alpha} = B(\mathbf{0}, \hat{r})$ , and  $\varepsilon = -1$  if  $\Omega_{\beta} = B(\mathbf{0}, \hat{r})$ . In that way, the outer unit normal  $\mathbf{n}$  to  $\Omega_{\alpha}$  equals  $\mathbf{n} = \varepsilon \mathbf{e}_r$ , where  $\mathbf{e}_r$  denotes a unit vector in a radial direction away from the origin.

The corresponding state  $u$  is also radial:  $u = u(r)$ , and consequently

$$\nabla u = u' \mathbf{e}_r, \quad \frac{\partial u}{\partial \mathbf{n}} = \varepsilon u',$$

i.e. the tangential derivative  $\nabla_{\Gamma} u$  vanishes on  $\Gamma$ .

The corresponding flux  $a \nabla u \in L^2(\Omega)$  has the form  $\sigma(r) \mathbf{e}_r$ , with  $\sigma = a u'$ , and the state equation (in two dimensions) turns to an ordinary differential equation for  $\sigma$ :  $-\frac{1}{r}(r\sigma)' = f$ . This equation has a unique solution in  $L^2(\Omega)$ :

$$\sigma(r) = -\frac{1}{r} \int_0^r \rho f(\rho) d\rho, \quad (8)$$

under the weak assumption  $r f(r) \in L^q((0, R))$ , for some  $q > 1$ , which follows from the minimal assumptions on  $f$  given in Remark 2. Moreover, in regions where  $f$  has  $H^1$  regularity, since it is a radial function, we have continuity of  $f$  (away from zero), implying that  $\sigma$  is derivable in these regions away from zero. The optimality conditions for the energy functional will be expressed solely in terms of  $\sigma$ .

The constraint on the amounts of the original phases is handled by the Lagrangian  $L(\Omega_{\alpha}) = J(\Omega_{\alpha}) - \lambda \text{vol}(\Omega_{\alpha})$ . The shape derivative of the volume functional is

$$\text{vol}'(\Omega_{\alpha}; \boldsymbol{\theta}) = \int_{\Gamma} \boldsymbol{\theta} \cdot \mathbf{n} dS,$$

or with regard to the first structure theorem,

$$l_1^{\text{vol}}(\phi) = \int_{\Gamma} \phi dS.$$

For the energy functional, in (4) we have

$$l_1^J(\phi) = \int_{\Gamma} \phi \llbracket \gamma \rrbracket \, dS.$$

Since the tangential gradient of  $u$  vanishes, we have

$$\gamma = a(u')^2 = \frac{\sigma^2}{a},$$

which leads to the first-order optimality condition

$$\frac{\beta - \alpha}{\alpha\beta} \sigma(\hat{r})^2 = \lambda. \quad (9)$$

In other words, the first-order optimality condition does not change if the phases  $\alpha$  and  $\beta$  change roles: both configurations  $\Omega_\alpha = B(\mathbf{0}, \hat{r})$  and  $\Omega_\beta = B(\mathbf{0}, \hat{r})$  are critical designs with the same Lagrange multiplier  $\lambda$ . Of course, the corresponding amounts  $q_\alpha$  of the first phase differ, but one easily calculates the corresponding  $\hat{r}$  in both configurations if  $q_\alpha$  is given, and by (9) the corresponding Lagrange multipliers follows.

In the sequel, we shall frequently use the notations  $u_\alpha$  and  $u_\beta$  for restrictions of the state function  $u$  to  $\Omega_\alpha$  and  $\Omega_\beta$ , respectively. The traces of these two functions on  $\Gamma$  will be denoted by the same letters. The same notation will be used for  $u'(\boldsymbol{\theta})$ . From (6) we see that  $u'$  actually depends only on the normal component of the perturbation  $\boldsymbol{\theta}$  on the interface  $\Gamma$ , so we shall write  $u' = u'(\boldsymbol{\theta} \cdot \mathbf{n}) = u'(\phi)$ .

For the second-order optimality condition, it is important to note that due to the second structure theorem, the expression for  $J'' - \lambda \text{vol}''$  for critical domains (those that satisfy the first-order optimality condition) simplifies to  $l_2^J - \lambda l_2^{\text{vol}}$ . These functionals can be written in the following form:

$$\begin{aligned} l_2^{\text{vol}}(\phi, \phi) &= \int_{\Gamma} H \phi^2 \, dS \\ l_2^J(\phi, \phi) &= \int_{\Gamma} \phi^2 \left\{ H \llbracket \gamma \rrbracket + \frac{\partial}{\partial \mathbf{n}} \llbracket \gamma \rrbracket \right\} \, dS \\ &\quad + 2\alpha \int_{\Gamma} \phi \left\{ \frac{\partial u_\alpha}{\partial \mathbf{n}} \frac{\partial u'_\alpha(\phi)}{\partial \mathbf{n}} - 2 \frac{\partial u_\alpha}{\partial \mathbf{n}} \nabla u_\alpha \cdot \nabla_{\Gamma} \phi - \nabla_{\Gamma} u_\alpha \cdot \nabla_{\Gamma} u'_\alpha(\phi) \right\} \, dS \\ &\quad - 2\beta \int_{\Gamma} \phi \left\{ \frac{\partial u_\beta}{\partial \mathbf{n}} \frac{\partial u'_\beta(\phi)}{\partial \mathbf{n}} - 2 \frac{\partial u_\beta}{\partial \mathbf{n}} \nabla u_\beta \cdot \nabla_{\Gamma} \phi - \nabla_{\Gamma} u_\beta \cdot \nabla_{\Gamma} u'_\beta(\phi) \right\} \, dS. \end{aligned}$$

In the spherically symmetric problem under consideration, in the last two rows in the expression above, only the first summand survives. Indeed, the second terms vanish since  $\nabla u_\alpha$  and  $\nabla u_\beta$  have a radial direction, which is orthogonal to tangential gradient  $\nabla_{\Gamma} \phi$ , while in the third summands tangential gradients  $\nabla_{\Gamma} u_\alpha$  and  $\nabla_{\Gamma} u_\beta$  vanish. Let us now calculate the difference  $l_2^J - \lambda l_2^{\text{vol}}$  for the Lagrange multiplier  $\lambda$  from (9):

$$\begin{aligned}
& (l_2^J - \lambda l_2^{\text{vol}})(\phi, \phi) \\
&= \int_{\Gamma} \phi^2 \frac{\partial}{\partial \mathbf{n}} [\gamma] \, dS + 2 \int_{\Gamma} \phi \left( \alpha \frac{\partial u_{\alpha}}{\partial \mathbf{n}} \frac{\partial u'_{\alpha}(\phi)}{\partial \mathbf{n}} - \beta \frac{\partial u_{\beta}}{\partial \mathbf{n}} \frac{\partial u'_{\beta}(\phi)}{\partial \mathbf{n}} \right) \, dS \\
&= \frac{\beta - \alpha}{\alpha \beta} \varepsilon (\sigma^2)'(\hat{r}) \int_{\Gamma} \phi^2 \, dS + 2\varepsilon \sigma(\hat{r}) \int_{\Gamma} \phi \left( \frac{\partial u'_{\alpha}(\phi)}{\partial \mathbf{n}} - \frac{\partial u'_{\beta}(\phi)}{\partial \mathbf{n}} \right) \, dS \quad (10) \\
&= 2\varepsilon \sigma(\hat{r}) \frac{\beta - \alpha}{\beta} \left( \frac{\sigma'(\hat{r})}{\alpha} \int_{\Gamma} \phi^2 \, dS + \int_{\Gamma} \phi \frac{\partial u'_{\alpha}(\phi)}{\partial \mathbf{n}} \, dS \right).
\end{aligned}$$

For the explicit calculation of this expression we use Fourier analysis. The first step is to solve the boundary value problem (6) with jump conditions by the Fourier separation method. In the case  $\varepsilon = 1$ , on the inner ball with radius  $\hat{r}$  we obtain

$$u'_{\alpha}(\phi) = \frac{A_0}{2} + \sum_{k=1}^{\infty} r^k (A_k \cos k\varphi + B_k \sin k\varphi),$$

while on the outer annulus, occupied by the better conductor, due to the boundary condition at  $r = R$  and we have

$$u'_{\beta}(\phi) = \sum_{k=1}^{\infty} \left( r^k - \frac{R^{2k}}{r^k} \right) (C_k \cos k\varphi + D_k \sin k\varphi).$$

If  $\varepsilon = -1$ , the above expressions for  $u'_{\alpha}$  and  $u'_{\beta}$  change place. Let us concentrate on the case  $\varepsilon = 1$ . The continuity of the flux implies

$$\begin{aligned}
& \alpha \sum_{k=1}^{\infty} k \hat{r}^{k-1} (A_k \cos k\varphi + B_k \sin k\varphi) \\
&= \beta \sum_{k=1}^{\infty} \left( k \hat{r}^{k-1} + k \frac{R^{2k}}{\hat{r}^{k+1}} \right) (C_k \cos k\varphi + D_k \sin k\varphi), \quad (11)
\end{aligned}$$

while the jump condition for  $u'(\phi)$  reads

$$\begin{aligned}
& \frac{A_0}{2} + \sum_{k=1}^{\infty} \hat{r}^k (A_k \cos k\varphi + B_k \sin k\varphi) \\
&= \frac{\alpha - \beta}{\alpha \beta} \sigma(\hat{r}) \phi + \sum_{k=1}^{\infty} \left( \hat{r}^k - \frac{R^{2k}}{\hat{r}^k} \right) (C_k \cos k\varphi + D_k \sin k\varphi). \quad (12)
\end{aligned}$$

Condition (11) implies

$$\begin{aligned}
A_k &= \frac{\beta}{\alpha} \left( 1 + \left( \frac{R}{\hat{r}} \right)^{2k} \right) C_k \\
B_k &= \frac{\beta}{\alpha} \left( 1 + \left( \frac{R}{\hat{r}} \right)^{2k} \right) D_k,
\end{aligned}$$



for  $k \in \mathbb{N}$ , so (12) can be rewritten as

$$\frac{\alpha - \beta}{\alpha\beta} \sigma(\hat{r}) \phi = \frac{A_0}{2} + \sum_{k=1}^{\infty} \left( \frac{\beta - \alpha}{\alpha} \hat{r}^k + \frac{\alpha + \beta}{\alpha} \frac{R^{2k}}{\hat{r}^k} \right) (C_k \cos k\varphi + D_k \sin k\varphi).$$

This implies that the coefficients  $C_k$  and  $D_k$  are determined by the Fourier coefficients of the function  $\phi$ : for  $k \in \mathbb{N}$  we have

$$C_k = \frac{(\alpha - \beta)\sigma(\hat{r})\mu_k}{\beta(\beta - \alpha)\hat{r}^k + \beta(\alpha + \beta)\frac{R^{2k}}{\hat{r}^k}}$$

$$D_k = \frac{(\alpha - \beta)\sigma(\hat{r})\nu_k}{\beta(\beta - \alpha)\hat{r}^k + \beta(\alpha + \beta)\frac{R^{2k}}{\hat{r}^k}},$$

where

$$\mu_k = \frac{1}{\pi} \int_0^{2\pi} \phi(\varphi) \cos k\varphi d\varphi, \quad k \in \mathbb{N}_0$$

$$\nu_k = \frac{1}{\pi} \int_0^{2\pi} \phi(\varphi) \sin k\varphi d\varphi, \quad k \in \mathbb{N}.$$

Finally, the second integral in (10) can be expressed as

$$\int_{\Gamma} \phi \frac{\partial u'_{\alpha}(\phi)}{\partial \mathbf{n}} dS = \hat{r}\pi \sum_{k=1}^{\infty} k \hat{r}^{k-1} (A_k \mu_k + B_k \nu_k)$$

$$= \hat{r}\pi \sigma(\hat{r}) \frac{\alpha - \beta}{\alpha} \sum_{k=1}^{\infty} \frac{k \left(1 + \left(\frac{R}{\hat{r}}\right)^{2k}\right)}{(\beta - \alpha)\hat{r} + (\alpha + \beta)\frac{R^{2k}}{\hat{r}^{2k-1}}} (\mu_k^2 + \nu_k^2),$$

and the first integral is

$$\int_{\Gamma} \phi^2 dS = \hat{r}\pi \left( \frac{\mu_0^2}{2} + \sum_{k=1}^{\infty} (\mu_k^2 + \nu_k^2) \right).$$

If  $\varepsilon = -1$ , one can easily adapt the previous calculation: in (11), the conductivities  $\alpha$  and  $\beta$  change place, while (12) remains the same. Of course, the same result can be easily obtained if one simply replaces the roles of  $\alpha$  and  $\beta$ . The final result is presented in the next theorem.

**Theorem 1.** *Let  $\Omega$  be a ball  $B(\mathbf{0}; R) \subseteq \mathbb{R}^2$ , the interface between the phases a sphere  $\partial B(\mathbf{0}; \hat{r})$ , with  $0 < \hat{r} < R$ , and  $f$  an outer heat source satisfying the assumptions of Remark 2. Then for  $\sigma$  given by (8) and  $\lambda = \frac{\beta - \alpha}{\alpha\beta} \sigma(\hat{r})^2$  the first-order necessary optimality condition is satisfied, and the second-order derivative of the Lagrangian is equal to*

$$(l_2^J - \lambda l_2^{\text{vol}})(\phi, \phi) = 2\pi\varepsilon\sigma(\hat{r}) \frac{\beta - \alpha}{\alpha\beta} \left[ \hat{r}\sigma'(\hat{r}) \left( \frac{\mu_0^2}{2} + \sum_{k=1}^{\infty} (\mu_k^2 + \nu_k^2) \right) \right. \\ \left. + \varepsilon(\alpha - \beta)\sigma(\hat{r}) \sum_{k=1}^{\infty} \frac{k(\hat{r}^{2k} + R^{2k})}{\varepsilon(\beta - \alpha)\hat{r}^{2k} + (\alpha + \beta)R^{2k}} (\mu_k^2 + \nu_k^2) \right], \quad (13)$$

where  $\mu_k$  and  $\nu_k$  stand for Fourier coefficients of the function  $\phi$ , and  $\varepsilon$  equals 1 if  $\Omega_\alpha = B(\mathbf{0}, \hat{r})$ , and  $-1$  if  $\Omega_\beta = B(\mathbf{0}, \hat{r})$ .

This result has several simple consequences. One can notice that the coefficients

$$\frac{k(\hat{r}^{2k} + R^{2k})}{\varepsilon(\beta - \alpha)\hat{r}^{2k} + (\alpha + \beta)R^{2k}} =: k\gamma_k \quad (14)$$

are positive, strictly increasing and unbounded, for both choices of  $\varepsilon$ , with coefficients  $\gamma_k$  uniformly positive. Moreover, the second summand in (13), multiplied by the corresponding factors, is negative for both configurations, unless  $\sigma(\hat{r})$  equals zero. This implies that any design with interface made of a single sphere such that  $\sigma(\hat{r}) \neq 0$  cannot lead to local minima for the energy functional. Furthermore, if the sign of  $\sigma'(\hat{r})$  is opposite to the sign of  $\varepsilon\sigma(\hat{r})$ , then we have the following coercivity property for the second-order derivative of the Lagrangian functional:

$$(l_2^J - \lambda l_2^{\text{vol}})(\phi, \phi) \leq -c\|\phi\|_{\mathbf{H}^{\frac{1}{2}}}^2, \phi \in \mathbf{H}^{\frac{1}{2}}(\partial\Omega), \quad (15)$$

for some positive constant  $c$ .

Otherwise, one should consider the sign of the first coefficient ( $k = 1$ ) in (13) to have a conclusion whether such coercivity holds. Namely, due to the presence of the volume constraint (3), the coercivity condition should be obtained only for perturbation fields  $\boldsymbol{\theta}$  which (locally) preserve the volume of  $\Omega_\alpha$ , meaning that the derivative  $\text{vol}'(\Omega_\alpha; \boldsymbol{\theta})$  equals zero, i.e.  $\int_\Gamma \phi = \frac{\hat{r}\pi}{2}\mu_0 = 0$ .

**Corollary 1.** *Under assumptions of Theorem 1 we have:*

1. *If  $\sigma'(\hat{r})$  and  $\varepsilon\sigma(\hat{r})$  have the opposite signs, then coercivity inequality (15) holds.*
2. *If  $\sigma'(\hat{r})$  and  $\varepsilon\sigma(\hat{r})$  are both positive or negative, then one calculates*

$$c(\hat{r}, \varepsilon) = \text{sign}(\varepsilon\sigma(\hat{r})) \left( \hat{r}\sigma'(\hat{r}) + \varepsilon(\alpha - \beta)\sigma(\hat{r}) \frac{(\hat{r}^2 + R^2)}{\varepsilon(\beta - \alpha)\hat{r}^2 + (\alpha + \beta)R^2} \right).$$

*If  $c(\hat{r}, \varepsilon) < 0$ , then (15) holds, and if  $c(\hat{r}, \varepsilon) > 0$ , then the corresponding design is not a point of local extrema.*

**Remark 3.** *As pointed out in [11] (see also [9]), coercivity condition (15) does not a priori imply that the critical design gives local maxima, since the coercivity is given in a weaker norm than the norm in which the functional is twice differentiable. In that paper, the authors consider the same energy functional, but for just one material (one conductivity degenerates to zero). However, in our situation, such result is technically more involved, and is still inaccessible. A general theory for this standard situation in shape optimization problems is presented in [10]. In the last section of our paper, a family of examples satisfying coercivity inequality (15) is numerically analyzed, confirming the appearance of local maxima.*

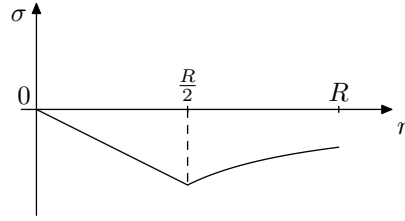


Figure 1: Graph of the function  $\sigma$  in Section 4.

### 4. Example

We shall present an application of the previous results for a piecewise constant (characteristic) right-hand side

$$f = \chi_{B(\mathbf{0}, \frac{R}{2})}.$$

As before, the quantity of the first phase is fixed to  $q_\alpha$ , and we shall also use the notation  $\eta = \frac{q_\alpha}{\text{vol}(\Omega_\alpha)} \in \langle 0, 1 \rangle$  for the overall fraction of the first phase.

In [29], the exact solution to this problem is presented by the method introduced in [22], via homogenization theory. The solution is unique and radial, and we have two possible optimal configurations:  $\Omega_\beta$  is an inner ball (if  $\eta \geq \frac{15}{16}$ ) or  $\Omega_\beta$  consists of an inner ball and an outer annulus (for other values of  $\eta$ ).

Let us check whether optimal design of the first kind is stable, and the possibility of existence of some other local maxima.

As before, if  $\Omega_\alpha$  or  $\Omega_\beta$  is a ball  $B(\mathbf{0}, \hat{r})$ , then the corresponding temperature  $u$  is a radial function, so the flux is of the form  $\sigma(r)\mathbf{e}_r$ , where  $\sigma$  solves

$$-\frac{1}{r}(r\sigma)' = \chi_{\langle 0, R/2 \rangle}, \quad r \in \langle 0, R \rangle.$$

This equation has a unique solution given by (8):

$$\sigma(r) = \begin{cases} -\frac{r}{2}, & 0 \leq r \leq \frac{R}{2} \\ -\frac{R^2}{8r}, & \frac{R}{2} \leq r \leq R, \end{cases}$$

with the graph presented in Figure 1.

Our aim is to consider simple critical designs, i.e. such with simple interface  $\Gamma$  made of just one sphere. Due to the expression for  $\sigma$ , we should consider the following four cases (due to Remark 2, we cannot consider the value  $\frac{R}{2}$  for  $\hat{r}$ ):

- A.  $\Omega_\alpha$  is a ball  $B(\mathbf{0}, \hat{r})$ , with  $0 < \hat{r} < \frac{R}{2}$
- B.  $\Omega_\alpha$  is a ball  $B(\mathbf{0}, \hat{r})$ , with  $\frac{R}{2} < \hat{r} < R$
- C.  $\Omega_\beta$  is a ball  $B(\mathbf{0}, \hat{r})$ , with  $0 < \hat{r} < \frac{R}{2}$
- D.  $\Omega_\beta$  is a ball  $B(\mathbf{0}, \hat{r})$ , with  $\frac{R}{2} < \hat{r} < R$

In each of the above cases, it is an easy task to explicitly calculate  $\hat{r}$  (if such exists) in terms of  $\eta$ . To be more precise, case A appears if and only if  $\eta < \frac{1}{4}$ , case B if and only if  $\eta > \frac{1}{4}$ , case C if and only if  $\eta > \frac{3}{4}$ , and case D appears if and only if  $\eta < \frac{3}{4}$ . Optimal design for  $\eta \geq \frac{15}{16}$  (the global maximizer), obtained in [29], fits case C.

As to the first part of Corollary 1, by using only the information on signs of  $\sigma$  and  $\sigma'$ , one concludes that cases B and C, for any admissible amount  $q_\alpha$  of the first phase, satisfy coercivity condition (15), potentially leading to local maxima (see Remark 3).

Cases A and D are analyzed by virtue of the second part of Corollary 1. A straightforward calculation gives

$$c(\hat{r}, 1) = \frac{\alpha R^2 \hat{r}}{(\beta - \alpha)\hat{r}^2 + (\alpha + \beta)R^2}$$

in case A, and

$$c(\hat{r}, -1) = \frac{2R^2(\alpha R^2 - (\beta - \alpha)\hat{r}^2)}{8\hat{r}(-(\beta - \alpha)\hat{r}^2 + (\alpha + \beta)R^2)}.$$

in case D. Therefore, case A does not lead to local extrema, while D satisfies (15) if and only if  $\alpha R^2 < (\beta - \alpha)\hat{r}^2$ .

## 5. Numerical example

Let the right-hand side in (1) be

$$f(r) = 6 - 6r,$$

on the unit circle in  $\mathbb{R}^2$ , with the corresponding flux

$$\sigma(r) = 2r^2 - 3r.$$

Qualitatively,  $\sigma$  is negative, strictly decreasing on  $[0, \frac{3}{4}]$  and strictly increasing on  $[\frac{3}{4}, 1]$ . Therefore, we shall consider the same cases A–D as in the previous example, but with  $R = 1$  and  $\frac{3}{4}$  instead of  $\frac{R}{2}$ . Additionally, due to the continuity of  $f$  we can analyze the case  $\hat{r} = \frac{3}{4}$ , which is simple:  $\sigma'(\hat{r}) = 0$  implies that in both configurations ( $\varepsilon = \pm 1$ ) coercivity condition (15) is satisfied.

Of course, for the given overall fraction  $\eta$  of the first phase, only some of these cases can appear. For example, in case B,  $\Omega_\alpha$  is a ball  $B(\mathbf{0}, \hat{r})$ , with  $\hat{r} > \frac{3}{2}$ , which implies that the corresponding  $\eta$  satisfies  $\eta > \frac{9}{16}$ . Similarly, case C appears only for  $\eta > \frac{7}{16}$ .

Since the assumptions of the first part in Corollary 1 are written in terms of sign of  $\sigma$  and  $\sigma'$ , the first conclusions are the same as in the previous example: cases B and C lead to inequality (15). Furthermore, cases A and D can be analyzed by the second part of Corollary 1.

One can apply [29, Lemma 2.6] to calculate unique optimal design: for  $\eta \geq \frac{3}{4}$ , optimal design fits case C, and otherwise, the best is to put a worse conductor  $\alpha$  in a middle annulus, surrounded by the better conductor  $\beta$ .

Let us numerically analyze case B, checking whether it leads to local maxima. As mentioned, the global maximum does not belong to that case, so we had to adjust the initial interface (closed to the desired one). We use the classical shape gradient method described in [18], see also [19]. Figures 2–4 deal with Lagrange multiplier  $\lambda = 0.625$ . The initial and the final design (after 200 iterations of the algorithm) are presented in Figure 2. We can see that the final design fits case B. The convergence history, presented in figures 3 and 4, confirms that we found a local maximum. A similar convergence occurs for different initial designs, as long as they are close to the spotted local maximum.

The presented example is not isolated. We tested the whole family of problems that fit case B. For different fixed Lagrange multipliers, after 200 iterations of the algorithm, we obtained (local) maxima by radial designs which fit case B, and we calculate the radius of the interface. These radii are presented in Figure 5, and the results perfectly fit the first-order necessary condition (9).

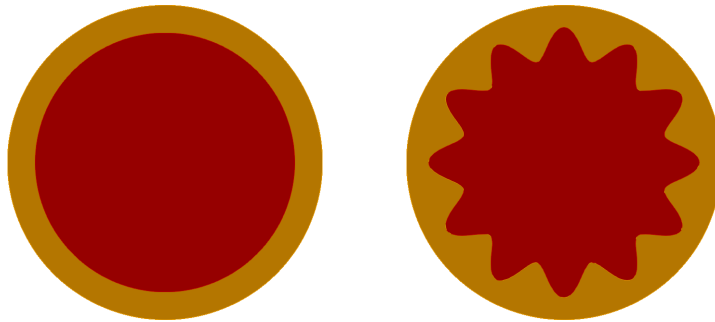


Figure 2: *The initial (left) and the final design (right). Red color represents the worse conductor ( $\alpha$ ), and yellow the better one ( $\beta$ ).*

## 6. Conclusion

Optimal design problems for stationary diffusion in the case of two isotropic phases aiming to maximize energy are well studied [22]. By relaxation via the homogenization approach developed there, for problems on a ball with spherically symmetric heat source [29], one is able to analyze the first-order optimality condition for the relaxed problem, leading to a unique maximizer which is radial and classical (i.e. the phases are split by a sphere or several spheres), except in some rare examples. However, by such relaxation the set of admissible designs is substantially enlarged by introducing fine mixtures of original phases. On the other hand, as is done in the methods based on shape differentiation, one could expect that by narrowing the set of admissible designs, some other local maxima could appear. In this paper, with an interface made of a single sphere, we investigate the optimality conditions based on the first- and second-order shape derivatives. Applying that analysis to an example, we obtained local maxima different from the global one. Such examples can

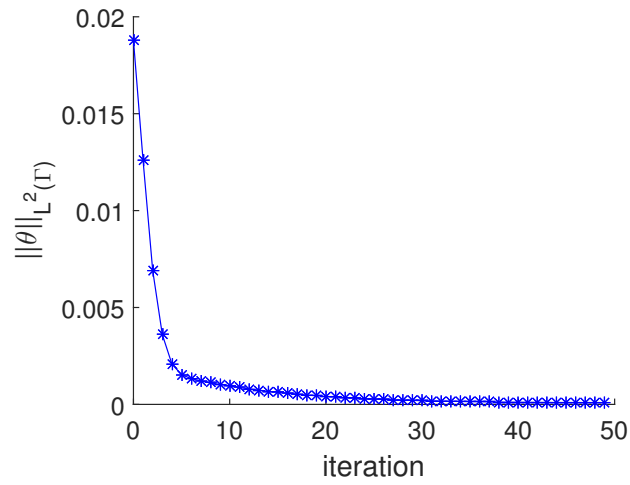


Figure 3:  $L^2$  norm of the perturbation field  $\theta$  with respect to the iteration number.

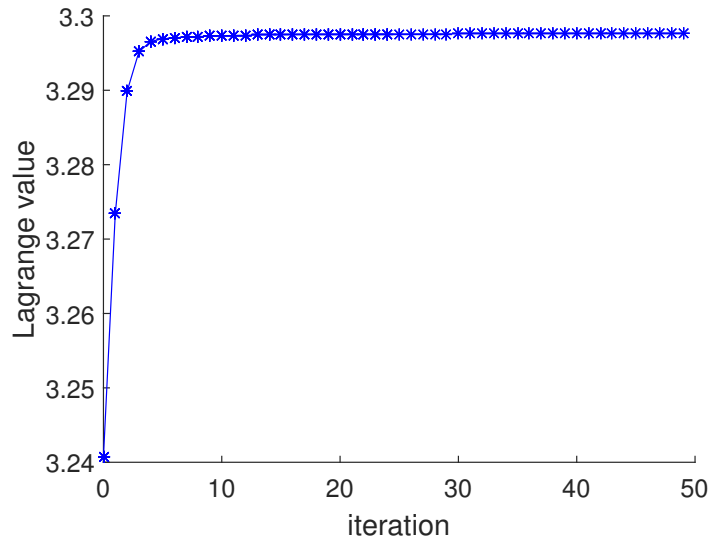


Figure 4: Value of the Lagrangian in terms of the iteration number.

be important in numerical simulations since algorithms based on shape derivatives could converge to such local maxima.

## Acknowledgement

The authors would like to thank the referees for their helpful suggestions.

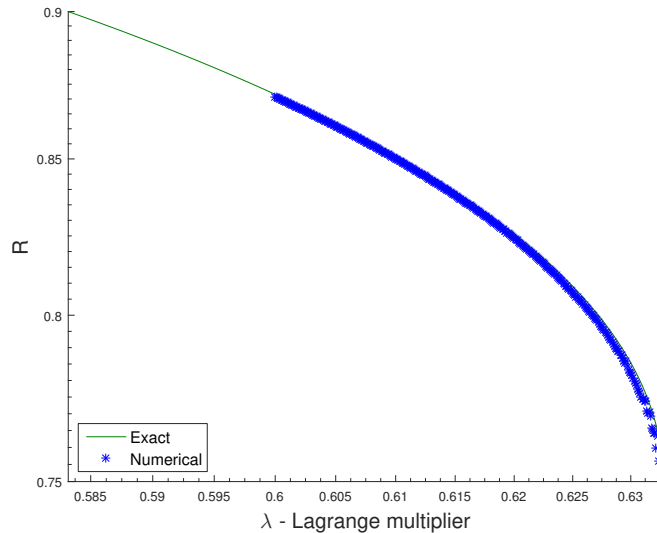


Figure 5: Dependence of the radius of the interface of calculated design on the Lagrange multiplier in case B, Subsection 4.2, and a comparison to exact values by formula (9).

## References

- [1] L. AFRAITES, M. DAMBRINE, D. KATEB, *Shape methods for the transmission problem with a single measurement*, Numer. Funct. Anal. Optim. **28**(2007), 519–551.
- [2] L. AFRAITES, M. DAMBRINE, D. KATEB, *On second order shape optimization methods for electrical impedance tomography*, SIAM J. Control Optim. **47**(2008), 1556–1590.
- [3] G. ALLAIRE, *Conception optimale de structures*, École polytechnique, Département de mathématiques appliquées, 2003.
- [4] L. AMBROSIO, G. BUTTAZZO, *An optimal design problem with perimeter penalization*, Calc. Var. Partial Differential Equations **1**(1993), 55–69.
- [5] C. BERNARDI AND O. PIRONNEAU, *Sensitivity of Darcy’s law to discontinuities*, Chin. Ann. Math. Ser. B **24**(2003), 205–214.
- [6] K. BURAZIN, M. VRDOLJAK, *Exact solutions in optimal design problems for stationary diffusion equation*, Acta. Appl. Math. **161**(2019), 71–88.
- [7] L. CAVALINA, *Locally optimal configurations for the two-phase torsion problem in the ball*, Nonlinear Anal. **162**(2017), 33–48.
- [8] J. CÉA, *Conception optimale ou identification de formes, calcul rapide de la dérivée directionnelle de la fonction coût*, Math. Mod. Numer. Anal. **20**(1986), 371–402.
- [9] M. DAMBRINE, *On variations of the shape Hessian and sufficient conditions for the stability of critical shapes*, RACSAM **96**(2002), 95–121.
- [10] M. DAMBRINE, J. LAMBOLEY, *Stability in shape optimization with second variation*, J. Differ. Equations **267**(2019), 3009–3045.
- [11] M. DAMBRINE, M. PIERRE, *About stability of equilibrium shapes*, ESAIM: M2AN **34**(2000), 811–834.
- [12] M. C. DELFOUR AND J.-P. ZOLÉSIO, *Shapes and Geometries: Analysis, Differential Calculus, and Optimization*, SIAM, 2001.
- [13] J. DESCLOUX, *An optimal design problem with perimeter penalization*, Z. Angew.

- Math. Phys. **45**(1994), 543–555.
- [14] J. HADAMARD, *Mémoire sur le problème d'analyse relatif à l'équilibre des plaques élastiques encastrées*, Imprimerie nationale, Vol. **33**, 1908.
  - [15] A. HENROT AND M. PIERRE, *Shape Variation and Optimization: A Geometrical Analysis*, EMS, 2018.
  - [16] F. HETTLICH AND W. RUNDELL, *The determination of a discontinuity in a conductivity from a single boundary measurement*, Inverse Problems **14**(1998), 67–82.
  - [17] P. KUNŠTEK, *Shape derivative techniques in optimal design*, PhD thesis, Faculty of Science, University of Zagreb, 2020.
  - [18] P. KUNŠTEK, M. VRDOLJAK, *Classical optimal designs on annulus and numerical approximations*, J. Differ. Equations **268**(2020), 6920–6939.
  - [19] P. KUNŠTEK, M. VRDOLJAK, *A quasi-Newton method in shape optimization for a transmission problem*, Optim. Methods Softw. **37**(2022), 2273–2299.
  - [20] A. LAURAIN, K. STURM, *Domain expression of the shape derivative and application to electrical impedance tomography*, Tech. Rep. 1863, 2013.
  - [21] F. MURAT, J. SIMON, *Sur le contrôle par un domaine géométrique*, Publication du Laboratoire d'Analyse Numérique de l'Université Paris **6**(1976), p. 189.
  - [22] F. MURAT, L. TARTAR, *Calcul des variations et homogénéisation*, Vol. **57**, Les Méthodes de l'Homogénéisation Théorie et Applications en Physique (Bréau-sans-Nappe, 1983); Collect. Dir. Études Rech. Élec. France, 1997, pp. 319–369.
  - [23] A. NOVRUZI, M. PIERRE, *Structure of shape derivatives*, J. Evol. Equ. **2**(2002), 365–382.
  - [24] A. PAGANINI, *Approximate shape gradients for interface problems*, in: New Trends in Shape Optimization, (A. Pratelli, G. Leugering, Eds.), International Series of Numerical Mathematics, Vol. **166**, Birkhäuser, 2015, 217–227.
  - [25] O. PANTZ, *Sensibilité de l'équation de la chaleur aux sauts de conductivité*, Cr. Acad. Sci. I-Math. **477**(2005), 275–337.
  - [26] J. SIMON, *Second variations for domain optimization problems*, in: Control theory of distributed parameter systems and applications, (M. Amouroux, A. El Jai, Eds.), Internat. Ser. Numer. Math., Vol. **91**, Birkhäuser, Basel, 1989, 361–378.
  - [27] K. STURM, *On shape optimization with non-linear partial differential equations*, PhD thesis, Technical University Berlin, 2015.
  - [28] J.-L. VIE, *Second-order derivatives for shape optimization with a level-set method*, PhD thesis, Université Paris Est, 2016.
  - [29] M. VRDOLJAK, *Classical optimal design in two-phase conductivity problems*, SIAM J. Control Optim. **54**(2016), 2020–2035.